Voxel-based Investigations of Phase Mask Effects on Susceptibility Weighted Images

Eo-Jin Hwang*, Min-Ji Kim[†], Hyug-gi Kim[†], Chang-Woo Ryu*, Geon-Ho Jahng*

*Department of Radiology, Kyung Hee University Hospital at Gangdong, School of Medicine, Kyung Hee University, Seoul, [†]Department of Biomedical Engineering, College of Electronic Information Engineering, Kyung Hee University, Yongin, Korea

To investigate effects of phase mask on susceptibility-weighted images (SWI) using voxel-based analyses in normal elderly subjects. A three-dimensional (3D) gradient echo sequence ran to obtain SWIs in 20 healthy elderly subjects. SWIs with two (SWI2) and four (SWI4) phase multiplications were achieved with positive (PSWI) and negative (NSWI) phase masks to investigate phase mask effects. The voxel-based comparisons were performed using paired t-tests between PSWI and NSWI and between SWI2 and SWI4. Differences of signal intensities between magnitude images and SWI4 were larger than those between magnitude images and SWI2s. Differences of signal intensities between magnitude images and PSWIs were larger than those between magnitude images and NSWIs. Moreover, the signal intensities from NSWI2s and NSWI4s were greater than those from PSWI2s and PSWI4s, respectively. More differences of signal intensities between NSWI4 and PSWI4s were found than those between NSWI2s and PSWI2s in the whole brain images. The voxel-based analyses of SWI could be beneficial to investigate susceptibility differences on the entire brain areas. The phase masking method could be chosen to enhance brain tissue contrast rather than to enhance venous blood vessels. Therefore, it is recommended to apply voxel-based analyses of SWI to investigate clinical applications.

Key Words: Susceptibility Weighted Imaging (SWI), Phase mask, Voxel-wise investigation

INTRODUCTION

Susceptibility-weighted imaging (SWI) is a magnetic resonance imaging technique[1] and is acquired using a three dimensionally fully flow-compensated gradient echo sequence to produce magnitude and phase images.[2,3] Paramagnetic substances such as iron, deoxyhemoglobin, methemoglobin, hemosiderin and ferritin cause positive phase shift, while diamagnetic substances such as calcium show negative phase shift.[4] The phase mask is thus conducted to suppress unwanted phase signals and enhance those from paramagnetic and diamagnetic sub-

stances and is multiplied by the magnitude images. The final SWI is created by combining magnitude images and phase masks. Susceptibility weighted imaging has been useful in observing aging effects in the normal human brains and in identifying a number of neurological disorders.[5-7] Those studies were performed with the region-of-interest (ROI)-based analysis rather than a voxel-based analysis.

The image contrasts and information illustrated on SWIs were varied by applying the post-processing steps to remove the phase values with low frequencies and by choosing a proper phase mask method with an optimal number of phase mask multiplications. Since the phase information takes an essential role in producing final SWIs, the post-processing steps to mask phase images and to combine them with magnitude images are crucial in extracting useful information and enhancing image contrasts. The phase values with low frequencies are usually removed during the post-processing steps by applying a high pass filter. Although the images are now without the inhomogeneity effects from the main field and tissue geometry,[2] it is still dif-

ficult to distinguish adjacent tissues with different susceptibilities because the images are influenced both by intra- and extra-tissue dephasing. The new phase images thus need to be masked in order to suppress phase values that are not in our interest. Because SWI is typically used to investigate venous blood effects, a phase masking method is usually chosen to enhance the vein contrast rather than enhance tissue contrast. If the vein looks bright in the phase images, a positive phase mask is chosen to enhance the vein signals; if the vein looks dark, the negative phase mask is used to do those. The masked phase images are then multiplied to the magnitude images to suppress pixels, enhancing the voxel values of the magnitude images. However, there are few studies to investigate SWI to enhance brain tissue contrast with minimizing dark vein signals.

The issues whether we need to have a positive phase mask or a negative one has previously been uninvestigated using the voxel-based analysis. Currently, voxel-based comparison analysis is well documented to investigate brain tissue alternations on three-dimensional (3D) T1-weighted (T1W) images. However, there are few studies on voxel-based changes of brain tissue on SWI. Therefore, the objective of this study was to investigate effects of the phase mask on SWIs using voxel-based analyses in normal elderly subjects. The phase mask effects were evaluated using two approaches. First, the SWIs processed by positive and negative phase masks were studied by comparing their signal differences. Second, the number of phase multiplication effects were investigated by performing voxel-wise comparisons among magnitude images and SWIs with two and four phase mask multiplications.

MATERIALS AND METHODS

1. Image acquisition

MR images were obtained in twenty healthy elderly human volunteers (mean age=67.8 years, standard deviation (SD)= 6.09 years, ranged from 62 to 80 years, 14 females and 6 males) who were no medical history of neurological diseases and was performed on a 3T MR system (Achieva, Philips Medical Systems, Best, The Netherlands) equipped with an eight-channel sensitivity encoding (SENSE) head coil. A fully first-order flow-compensated 3D gradient echo sequence ran to obtain axial magnitude and phase images to generate SWI. The following parameters were used: repetition time (TR)=24 ms, echo time (TE)=34 ms, flip angel=8°, field-of-view (FOV) =236×236 mm, acquisition voxel size=0.63×0.63×1.26 mm^3, and reconstructed voxel size=0.47×0.47×0.63 mm^3, which was later reconstructed to 1×1×1 mm^3 for post- processing. In addition, sagittal structural 3D T1W images were acquired with the magnetization-prepared rapid acquisition of gradient echo (MPRAGE) sequence for imaging registration to the brain anatomy template. The imaging parameters used were as follows: TR=8.1 ms, TE=3.7 ms, flip angel=8°, FOV=236×236 mm^2, and voxel size=1×1×1 mm^3.

2. Post-processing

The post-processing step to create final SWI was performed using SPIN software (Wayne State University, MI, USA. http://www.mrc.wayne.edu/download.htm). The phase images were filtered by using a 64×64 Hz high pass filter to diminish a low frequency components,[2] which was followed by a masking process; a positive phase mask was performed to linearly scale all the positive phase values from 0 to 1 and to assign 1 for those less than 0 because vein signals in phase images appeared in our case. Additionally, to compare images generated from the positive phase mask, a negative phase mask was also performed to the same high-pass filtered phase images to linearly scale all the negative phase values from 0 to 1 and to assign 1 for those greater than 0. Because the negative phase mask enhanced a few soft tissues while suppressing vein signals, it is assumed to reduce the susceptibility effects revealed in the SWI. The magnitude images were then multiplied by the positive and negative phase masks twice[2] and four[4] times, to create positively phase-masked SWI2 (PSWI2) and SWI4 (PSWI4), and negatively phase-masked SWI2 (NSWI2) and SWI4 (NSWI4), respectively.

The following co-registration, normalization, and smoothing steps were achieved using a Statistical Parametric Mapping-version 5 (SPM5) program (Wellcome Department of Imaging Neuroscience, University College, London, UK). For each subject, the 3D T1W images were co-registered with the magnitude images. The 3D T1W images were then spatially normalized to a Korean standard structural brain template for the elderly,[8] which was created by averaging 123 brains of the eld-

erly (mean age=68.2, SD=8.6), using a 12-parameter nonlinear transformation. The same transformation parameters of 3D T1W images were applied to normalize magnitude, high-pass filtered phase, PSWI2 and PSWI4, and NSWI2 and NSWI4 which were interpolated to the 1 mm×1 mm×1 mm voxel size of the brain template. Magnitude images, SWI2 and SWI4 were smoothed using a 4×4×4 mm^3 Gaussian kernel to perform voxel-based comparisons in SPM5.

3. Statistical analyses

All voxel-based statistical analyses were also achieved using SPM5 software. In order to investigate *multiplication effects of phase*, the voxel-based comparisons of the whole brain images were performed using the paired t-tests between magnitude and PSWI2, between magnitude and PSWI4, between PSWI2 and PSWI4, between magnitude and NSWI2, between magnitude and NSWI4, and between NSWI2 and NSWI4. The family-wise error rate (FWE) was applied to account for the multiple comparisons, and a threshold for the significance of FWE p=0.0000000001 was chosen with a threshold looking for clusters with at least 10 contiguous voxels. The gender and age

information of the subjects were included as covariates.

In order to investigate *phase-mask effects*, the voxel-based comparisons were also performed using a paired t-test between SWIs processed by the positive phase mask and that by negative one. Therefore, in these analyses, we compared between NSWI2 and PSWI2 and between NSWI4 and PSWI4 in the entire brains. The threshold for the significance was p=0.005 with FWE for the multiple comparisons with a threshold looking for clusters with at least 10 contiguous voxels. The information on gender and age were also included as covariates.

To investigate regional differences in specific brain areas rather than the whole brain, the ROI-based analysis was performed with different regions of interest (ROIs). The anatomical ROIs that are known for rich iron-contents were selected based on the previous studies on detecting rich iron-content regions of the brain (Haacke et al, 2005) using a WFU Pick-Atlas software (Wake Forest University School of Medicine, USA). The following ROIs were selected; Amygdala, Globus Pallidus, Hippocampus, Pulvinar, Putamen, Red Nucleus, Thalamus and Precaneus. The average signal intensities from the selected ROIs were calculated using a Marsbar software
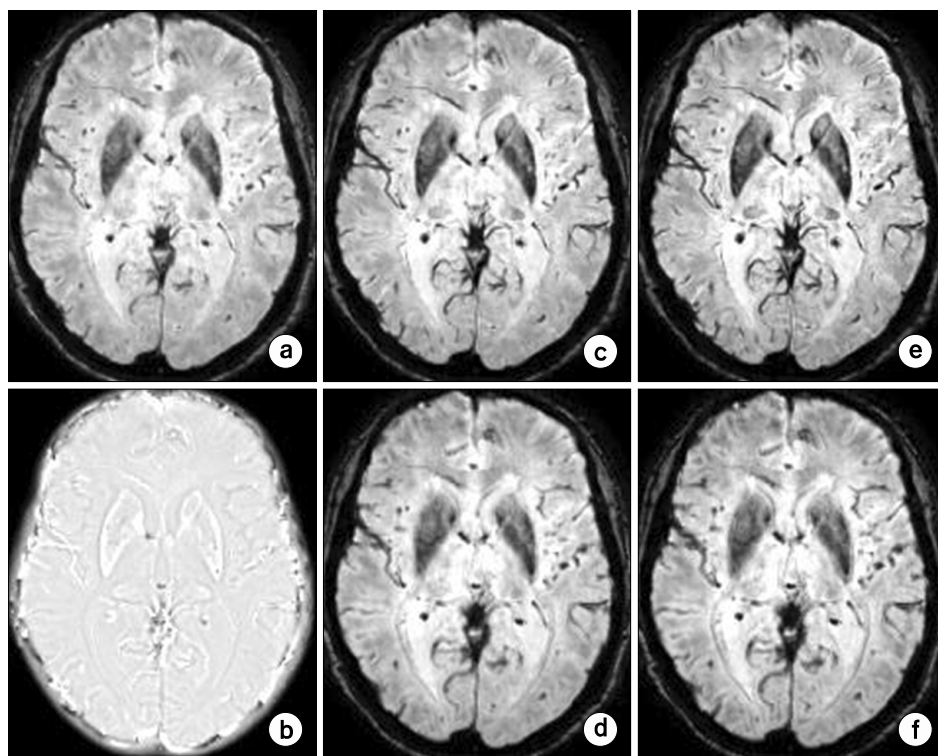
Fig. 1. The representative whole brain images obtained from a healthy human subject. Magnitude (a), phase (b), positively phase-masked susceptibility-weighted image (SWI) with 2 phase mask multiplications (PSWI2, c), negatively phase-masked SWI with 2 phase mask multiplications (NSWI2, d), positively phase-masked SWI with 4 phase mask multiplications (PSWI4, e), negatively phase-masked SWI with 4 phase mask multiplications (NSWI4, f).

(Matthew Brett, http://marsbar.sourceforge.net/), and a statistical analysis of the collected mean values for each ROI was performed by generating a one-way analysis of variance (ANOVA) test to compare differences among the image types (magnitude, SWI2 and SWI4, Degree of freedom (DOF)=2), between different phase mask effects (positive vs. negative phase mask, DOF=1), between brain tissue masking effects (with vs. without brain tissue mask, DOF=1), and among the selected ROIs (DOF=10). A post-hoc analysis was subsequently performed for those showing significant differences, where the Turkey method was used for multiple comparisons of image types and ROIs, while the LSD method was used for multiple comparisons of tissue masking effects.

RESULTS

The representative whole brain magnitude image, phase image, PSWI2, NSWI2, PSWI4 and NSWI4 are shown in Fig. 1. It is to be noted that the susceptibility image contrast increases from the magnitude image to PSWI2 and to PSWI4; in addition, PSWI2 and PSWI4 revealed better image contrasts than NSWI2 and NSWI4, respectively. Susceptibility image contrast is the greatest in PSWI4 and is the weakest in the magnitude image. The contrasts were better in PSWI2 and PSWI4 than in NSWI2 and NSWI4, respectively.

The results of voxel-wise comparisons between magnitude images and positively phase-masked SWI are shown in Fig. 2. Magnitude images produced the highest signals compared to those from PSWI2 and PSWI4, and more differences were found between magnitude and PSWI4 than between magnitude and PSWI2. The main differences were found on the left and right culmen, on the right lingual gyrus, and on the left and right claustrum. The Talairach coordinates and anatomical information corresponding to the regions showing differences with T-score higher than 37 are summarized in Table 1. No significant difference was found between PSWI2 and PSWI4.

The results of voxel-wise comparisons between magnitude and negatively phase-masked SWI are shown in Fig. 3. Magnitude images produced the highest signals compared to those from NSWI2 and NSWI4, and more differences were found between magnitude and NSWI4 than between magnitude and NSWI2. The main differences were found on the left pre-

central gyrus, left paracentral lobule, left medial frontal gyrus, left red nucleus and on the right lingual gyrus. The Talairach coordinates and anatomical information corresponding to the regions showing differences with T-score higher than 37 are summarized in Table 2. In addition, slight differences were found between NSWI2 and NSWI4, mainly on the left putamen, the right medial globus pallidus, the right culmen, and the right red nucleus. It is to be noted that more voxel-wise differences were found between magnitude and PSWIs than between that and NSWIs.

The results of voxel-wise comparisons between the positive phase mask and the negative phase mask are shown in Fig. 4. Signals from NSWI2 and NSWI4 were greater than those from PSWI2 and PSWI4, respectively, and more differences were found when comparing NSWI4 and PSWI4 than comparing NSWI2 and PSWI2 in the whole brain images. The main differences were found on the left and right caudate, the left and right lateral globus pallidus, the right red nucleus and the left and right anterior cingulate. The Talairach coordinates and anatomical information corresponding to the regions showing differences with T-score higher than 14 are summarized in Table 3.

The one-way ANOVA test showed that the significant differences existed among the different image types (F=125.93,

Fig. 2. Results of voxel-wise comparisons between magnitude images and *positively* (P) phase-masked susceptibility weighted images (SWIs) with two different phase mask multiplications. Comparison between magnitude images and *positively* phase-masked SWI with 2 phase mask multiplications (magnitude > PSWI2, a) and between magnitude images and *positively* phase-masked SWI with 4 phase mask multiplications (magnitude > PSWI4, b). No significant differences were found between P_SWI2 and P_SWI4.

p=0.00000001), among the selected ROIs (F=101.88, p=0.00000001) and between brain tissue-masking effects (F=748.96, p= 0.00000001), but not for positive-negative phase mask (F= 2.8151, p=0.0934792). A post-hoc analysis revealed that the significant differences lied between magnitude images and SWI2, between magnitude and SWI4 and between SWI2 and SWI4.

Table 1. Anatomical regions showing significant differences between magnitude and positively (P) phase-masked susceptibility-weighted imaging (SWI).

Anatomy	Magnitude＞PSWI2				Magnitude＞PSWI4			
	Talairach coordinate			T−score	Talairach coordinate			T−score
	x	y	z	T	x	y	z	T
R. Culmen	6.35	−47.78	−6.45	41.98	6.35	−47.78	−6.45	40.56
					5.29	−69.72	−3.14	40.31
					8.15	−51.77	−4.09	39.86
L. Culmen	−8.46	−59.55	−10.52	39.06	−8.45	−44.9	−6.43	42.17
	−16.8	−61.46	−9.94	39.57				
R. Dendate					14.86	−56.5	−23.35	52.37
R. Superior Frontal Gyrus					4.91	17.89	52.9	50.22
					3.84	9.57	61.1	37.45
R. Medial Frontal Gyrus					3.78	−7.37	61.3	37.92
L. Medial Frontal Gyrus					3.03	−16.13	45.14	37.15
R. Precentral Gyrus					49.37	−11.28	41.88	45.31
					34.33	−27.5	54.5	38.28
R. Paracentral Lobule					3.03	−16.13	45.14	37.15
L. Paracentral Lobule					−3.57	−24.25	51.47	46.32
					−3.68	−32.4	57.9	41.31
R. Parahippocampal Gyrus	16.77	−16.8	−15.95	44.35				
L. Sub-Gyral	−23.16	−18.48	−6.87	38.76				
R. Anterior Cingulate					1.88	32.95	4.73	37.79
L. Anterior Cingulate	−24.05	33.84	6.18	38.25				
R. Uncus					28	−5.82	−22.83	40.38
R. Lingual Gyrus	8	−78.47	−0.32	39.77	8.91	−78.56	0.59	46.72
					1.5	−70.4	3.94	38.04
R. Red Nucleus					6.49	−19.3	−9.15	45.95
R. Postcentral Gyrus					38.93	−34.13	54.85	46.11
					19.44	−38.11	57.75	43.89
					34.52	−21.54	41.56	37.22
L. Postcentral Gyrus					−31.4	−31.06	54.85	39.07
R. Inferior Parietal Lobule					37.11	−45.8	49.21	37.46
R. Cerebellar Tonsil					26.06	−65	−32.97	41.27
L. Cerebellar Tonsil	−12.73	−49.63	−34.87	37.82				
R. Declive					38.84	−59.94	−17.86	41.57
R. Medial Globus Pallidus	12.01	−4.02	−2.21	48.89				
R. Claustrum	26.75	15.53	8.9	39.53	37.02	−2.11	−3.4	38.1
L. Claustrum	−33.29	−11.65	−9.1	39.21	−35.19	−18.42	−7.07	40.26
L. Putamen	−20.57	−2.54	12.7	41.85				
L. Medial Globus Pallidus					−10.14	−0.76	−5.88	49.49
L. Thalamus	0.79	0.67	7.96	39				
	−15.01	−13.48	9.05	38.23				
L. Inferior Temporal Gyrus					−44.63	−53.54	−3.35	48.49
L. Superior Temporal Gyrus					−35.52	−31.86	15.07	43.63
L. Sub-Gyral					−42.53	−4.23	−7.65	39.91
					−33.36	−25.88	−7.75	37.38

After the threshold with family-wise error rate (FWE) p=0.0000000001 as the cluster level, only the Talairach coordinates with T-score greater than 37 are indicated on the list.
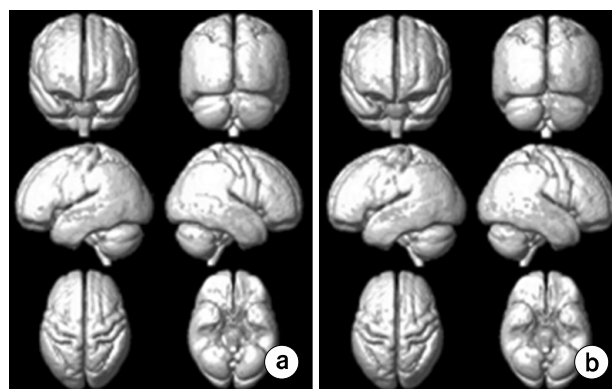R: Right, L: Left, SWI2: SWI with 2 phase mask multiplications, SWI4: SWI with 4 phase mask multiplications.
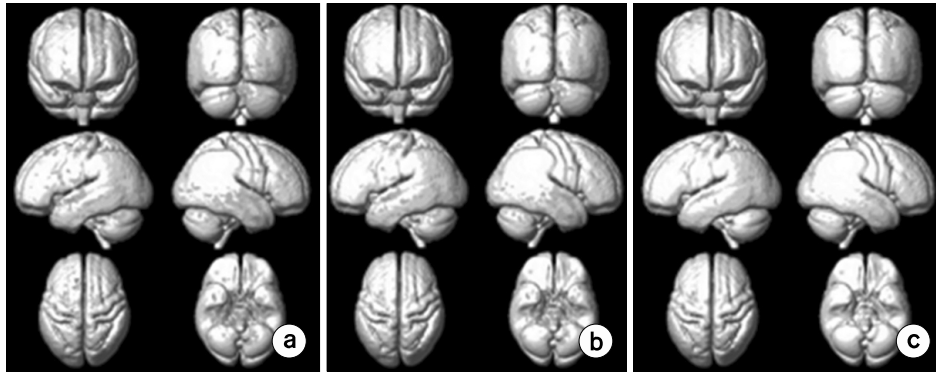
Fig. 3. Results of voxel-wise comparisons between magnitude images and negatively (N) phase- masked susceptibility weighted image (SWI) with two different phase mask multiplications. Comparisons between magnitude images and *negatively* phase-masked SWI with 2 phase mask multiplications (magnitude＞NSWI2, (a), between magnitude images and *negatively* phase-masked SWI with 4 phase mask multiplications (magnitude＞NSWI4, (b), and between NSWI2 and NSWI4 (NSWI2＞NSWI4, c).

Table 2. Anatomical regions showing significant differences between magnitude and negatively (N) phase-masked susceptibility-weighted imaging (SWI).

| Anatomy | Magnitude＞NSWI2 | | | | Magnitude＞NSWI4 | | | |
| | Talairach coordinate | | | T-score | Talairach coordinate | | | T-score |
	x	y	z	T	x	y	z	T
R. Culmen	7.21	−53.72	−3.39	43.17	17.67	−27.89	−17.89	45.43
					9.1	−47.03	−4.53	40.29
					8.48	−35.62	−25.08	39.03
R. Nodule	3.85	−56.68	−30.76	37.2	3.84	−57.61	−30.84	37.88
L. Nodule	−4.5	−57.65	−30.09	38.21				
R. Precentral Gyrus	49.53	−2.78	31.88	38.67				
L. Precentral Gyrus	−49.48	−2.18	29.36	37.6	−49.48	−1.25	29.45	38.93
	−17.46	−23.33	52.22	40.46	−17.44	−23.24	51.33	37.74
R. Paracentral Lobule	18.53	−40.72	55.68	37.12				
L. Paracentral Lobule	−17.58	−38.85	57.05	37.17	−9.17	−33.71	52.28	39.28
L. Medial Frontal Gyrus	−10.18	−25.41	53.95	56.24	−9	−26.25	52.95	47.73
	−15.45	9.79	49.99	38.07				
L. Cingulate Gyrus	7.88	−16.28	27.19	39.93				
R.Parahippocampal Gyrus					19.68	−13.06	−25.45	37.22
L. Parahippocampal Gyrus	−25.91	−21.93	−9.95	39.48				
R. Anterior Cingulate					8.98	12.36	22.72	38.85
L. Red Nucleus	−2.88	−21.9	−1.45	39.59	−2.88	−21.9	−1.45	43.41
R. Lingual Gyrus	7.07	−81.26	−0.6	38.96	7.07	−81.26	−0.6	45.67
L. Lingual Gyrus	−6.83	−88.64	−1.53	37.5				
	−7.65	−85.99	−9.4	37.38				
R. Cerebellar Tonsil					8.56	−50.59	−35.5	38.15
L. Uvula					−13.81	−62.61	−27.11	38.88
R. Lateral Globus Pallidus					20.4	0.01	−5.29	48.58
					21.19	−15.59	0.46	43.29
L. Lateral Globus Pallidus					−24.09	−10.27	−4.31	40.91
R. Putamen					25	−2.89	−4.58	44.78

After the threshold with family-wise error rate (FWE) p=0.0000000001 as the cluster level, only the Talairach coordinates with T-score greater than 37 are indicated on the list.
R: Right, L: Left, SWI2: SWI with 2 phase mask multiplications, SWI4: SWI with 4 phase mask multiplications.
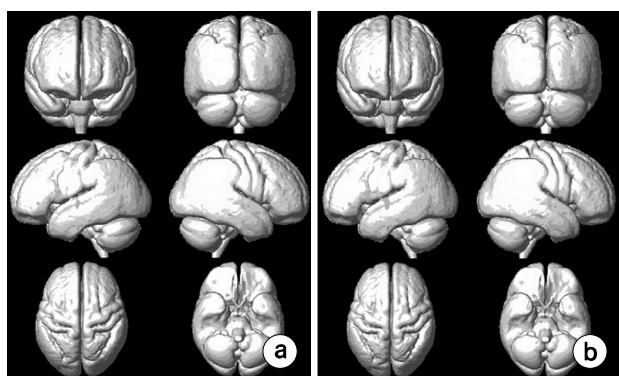
DISCUSSION

The main objective of this study was to investigate phase mask effects on SWI in the voxel-based analysis. Because the post-processing step to utilize a phase image is crucial in creating final images, the image contrasts differ by which a method is chosen to be processed. Therefore, it is important to examine differences among SWIs produced by different phase masking methods and to observe how the utilization of masking methods affects final image contrasts. Throughout the study, the signal variations between SWIs created by positive phase masks, which led to enhance signals from venous blood veins, and those by negative phase masks, which enhanced some tissue contents having negative phase values, were compared. The number of phase mask multiplication effects was also studied by comparing SWIs with two multiplications and those with four multiplications. The major findings of this study were the following; first, the general signal intensity val-

Fig. 4. Results of voxel-wise comparisons between susceptibility-weighted imaging (SWI) with the *positive* (P) phase mask and that with the *negative* (N) phase mask with the whole brain with the threshold of family-wise error rate (FWE) p=0.005. (a) Comparison between the whole brain negatively phase-masked SWI with 2 phase mask multiplications and *positively* phase-masked SWI with 2 phase mask multiplications (NSWI2> PSWI2). (b) Comparison between the whole brain *negatively* phase-masked SWI with 4 phase mask multiplications and *positively* phase-masked SWI with 4 phase mask multiplications (NSWI4>PSWI4).

Table 3. Anatomical regions showing significant differences between the whole brain susceptibility-weighted imaging (SWI) with the positive (P) phase mask and that with the negative (N) phase mask.

Anatomy	NSWI2>PSWI2 Talairach coordinate x	y	z	T-score T	NSWI4>PSWI4 Talairach coordinate x	y	z	T-score T
L. Anterior Cingulate	−9.15	26.25	−3.3	14.04				
	−8.18	34.8	−4.27	16.73	−2.69	10.55	−6.48	17.13
R. Anterior Cingulate	2.86	16.87	−3.99	14.58	4.72	17.88	−4.76	15.96
R. Red Nucleus	5.55	−19.39	−8.28	14.92	5.55	−18.46	−8.19	17.93
L. Lateral Globus Pallidus	−25.06	−14.25	−2	15.64	−25.96	−14.07	−3.8	22.56
					−26.08	−14.94	5.12	19.96
					−24.19	7.23	9.06	15.51
R. Lateral Globus Pallidus	23.99	−13.57	−1.11	16.7	24.92	−14.51	−1.18	19.11
					24.81	−14.36	6.94	16.51
L. Caudate	−12.18	7.93	11.13	17.6	−12.18	7	11.04	16.01
					9.29	−0.86	−5.56	14.61
	−2.77	13.58	1.01	15.62	−4.61	16.48	0.36	18.76
R. Caudate	10.06	6.21	8.64	16.1	10.93	7.63	13.29	18.47
	15.53	17.23	10.68	14.49	16.53	16.16	12.39	17.65
Thalamus					5.45	−18.31	−0.07	15.5
					−11.17	−13.39	−1.68	15.46
					10.1	−12.66	−0.35	14.19
Cerebellar Tonsil					0.22	−51.56	−34.84	14.78

After the threshold with family-wise error rate (FWE) p=0.005 as the cluster level, only the Talairach coordinates with T-score greater than 14 are indicated on the list.
R: Right, L: Left, SWI2: SWI with 2 phase mask multiplications, SWI4: SWI with 4 phase mask multiplications.

ues decreased as the number of phase mask multiplications increased, and second, positively phase-masked SWIs revealed lower signal intensities compared to those in negatively phase-masked SWIs, indicating that emphasizing venous blood signals attributed to more contrasts in SWI.

When magnitude, SWI2 and SWI4 were compared using voxel-based analyses, the signal intensity diminished from magnitude to SWI2 and to SWI4 both in PSWIs and NSWIs. This is because increasing phase mask multiplications caused more signal loss in final SWIs, from which the original magnitude image was weighed by dephasing of the phase signals. The final SWI, which was a product of magnitude and phase images, revealed the regions with darker signals, highlighting the susceptibility effects within the images. The more the signals were lost, the larger the voxel numbers showing variances with the magnitude images. From the above results, we can conclude that 4 multiplications created more signal loss than 2 multiplications due to the enhanced susceptibility effects exposed in the phase images, which produced more contrasts in SWIs. Additionally, variances also existed among magnitude images and SWI2 and SWI4 when the same voxel-based analyses were performed. This indicates that dephasing effects also existed within the tissue contents of the brain and that the factors causing susceptibility effects were not limited to the venous blood vessels, which is consistent with the findings from previous researches. Haacke et al. demonstrated that the phase multiplication of 4 produced the most optimal contrast-to-noise ratio (CNR) in SWI,[2] and many previous researches on SWI have chosen 4 multiplications to phase mask in detecting iron contents[10,11] during their ROI-based analyses. Chamberlain et al., on the other hand, have chosen 5 multiplications to display amyloid plaque.[12] In short, the susceptibility effects were enhanced with increasing number of phase mask multiplications and were not limited to the paramagnetic substances within venous blood vessels.

Our results also showed that PSWIs had lower signal intensities than NSWIs, which indicated that enhancing phase signals from venous blood veins using positive phase masks revealed better susceptibility effects in final SWIs. On the other hand, because negatively masked SWIs enhanced only negative phase signals present in soft tissues, the susceptibility effects were not as much boosted as those in the positi-

vely-masked SWIs. Therefore, the resulting signal intensities were greater in negatively-masked SWI due to the lesser amount of susceptibility effects weighed. While negative masks weakened the signals from venous blood vessels influenced by the susceptibility effects, the negative phase masks, which reduced signals in soft tissues, revealed less susceptibility effects by producing relatively high signal intensities. Therefore, we could conclude that SWIs created by the positive phase masks, which enhanced the phase signals from venous blood vessels in our case, were more sensitive to susceptibility effects than those created by the negative phase masks. However, the positive or negative phase mask is dependent on the type of imaging sequences for each vendor. Therefore, our result can support for the scanner vendor in this study.

The results of voxel-wise comparisons between the whole brain NSWI and PSWI showed that more differences lied between NSWI4s and PSWI4s than between NSWI2s and PSWI2s. This is because the signal intensities were reduced as the number of phase-mask multiplications increased. Because the positive phase masks are known to be more sensitive to susceptibility effects as previously mentioned in this study, the higher number of mask multiplications would have caused more signal losses in final PSWIs; conversely, because the NSWIs were less sensitive to susceptibility effects, the increasing number of mask multiplications would not have significantly influenced in signal losses due to the magnetic susceptibility. The differences between NSWI and PSWI would have thus augmented as the phase mask multiplications were performed four times.

One limitation of this study was the uncertain relationship between phase signals and the susceptibility effects. Although phase images contain information on susceptibility differences, the phase contrast does not fully correspond to the susceptibility differences; therefore, one cannot easily conclude that the final SWIs produced by phase mask multiplications purely enhanced the susceptibility effects. It is thus important to quantify and solely extract the susceptibility information from the acquired phase images.[3,13-15] Therefore, the future studies on magnetic susceptibility using SWI should be benefited from these quantitative susceptibility maps, which exclusively reveal the susceptibility values within the voxels. Finally, Haacke et al investigated filtering size effects on SWI,[2] but we only ap-

plied the central filter size of 64×64 in this study without investigating voxel-based SWI affected by the filter sizes. It has been studied that the most optimal filter size for measuring iron contents was 64×64, since filtering sizes greater than 64 may remove some important physiologically or pathologically important information.[2]

CONCLUSION

Our study suggests that the voxel-based analysis of SWI data could be beneficial to investigate susceptibility differences on the entire brain areas. Choosing 4 phase mask multiplications produced better image contrasts than conducting 2 phase mask multiplications. The phase masking method can be chosen to enhance brain tissue contrast rather than to enhance venous blood vessels. Thus, voxel-based analysis of SWI should be applied to investigate various clinical cases.

REFERENCES

1. Haacke EM, Xu Y, Cheng YC, Reichenbach JR: Susceptibility weighted imaging (SWI). Magn Reson Med 52(3):612–618 (2004)

2. Haacke EM, Mittal S, Wu Z, Neelavalli J, Cheng YC: Susceptibility-weighted imaging: technical aspects and clinical applications, part 1. AJNR Am J Neuroradiol 30(1):19–30 (2009)

3. Rauscher A, Sedlacik J, Barth M, Mentzel HJ, Reichenbach JR: Magnetic susceptibility-weighted MR phase imaging of the human brain. AJNR Am J Neuroradiol 26(4):736–742 (2005)

4. Haacke EM, Cheng NY, House MJ, et al: Imaging iron stores in the brain using magnetic resonance imaging. Magn Reson Imaging 23(1):1–25 (2005)

5. Xu X, Wang Q, Zhang M: Age, gender, and hemispheric differences in iron deposition in the human brain: an in vivo MRI study. Neuroimage 40(1):35–42 (2008)

6. Pfefferbaum A, Adalsteinsson E, Rohlfing T, Sullivan EV: MRI estimates of brain iron concentration in normal aging: comparison of field-dependent (FDRI) and phase (SWI) methods. Neuroimage 47(2):493–500 (2009)

7. Haacke EM, Miao Y, Liu M, et al: Correlation of putative iron content as represented by changes in R2* and phase with age in deep gray matter of healthy adults. J Magn Reson Imaging 32(3):561–576 (2010)

8. Kim MJ, Jahng GH, Lee HY, et al: Development of a Korean standard structural brain template in cognitive normals and patients with mild cognitive impairment and Alzheimer's disease. J Korean Soc Magn Reson Med 14(2):103–114 (2010)

9. Maldjian JA, Laurienti PJ, Kraft RA, Burdette JH: An automated method for neuroanatomic and cytoarchitectonic atlas-based interrogation of fMRI data sets. Neuroimage 19(3):1233–1239 (2003)

10. Eissa A, Lebel RM, Korzan JR, Catz I, et al: Detecting lesions in multiple sclerosis at 4.7 tesla using phase susceptibility-weighting and T2-weighting. J Magn Reson Imaging 30(4):737–742 (2009)

11. Grabner G, Dal-Bianco A, Schernthaner M, Vass K, Lassmann H, Trattnig S: Analysis of multiple sclerosis lesions using a fusion of 3.0 T FLAIR and 7.0 T SWI phase: FLAIR SWI. J Magn Reson Imaging 33(3):543–549 (2011)

12. Chamberlain R, Reyes D, Curran GL, et al: Comparison of amyloid plaque contrast generated by T2-weighted, T2*-weighted, and susceptibility-weighted imaging methods in transgenic mouse models of Alzheimer's disease. Magn Reson Med 61(5):1158–1164 (2009)

13. Niwa T, Aida N, Kawaguchi H, et al: Anatomic dependency of phase shifts in the cerebral venous system of neonates at susceptibility-weighted MRI. J Magn Reson Imaging 34(5):1031–1036 (2011)

14. Shmueli K, de Zwart JA, van Gelderen P, Li TQ, Dodd SJ, Duyn JH: Magnetic susceptibility mapping of brain tissue in vivo using MRI phase data. Magn Reson Med 62(6):1510–1522 (2009)

15. Schafer A, Wharton S, Gowland P, Bowtell R: Using magnetic field simulation to study susceptibility-related phase contrast in gradient echo MRI. Neuroimage 48(1):126–137 (2009)

화소 간 분석을 이용하여 자화율 가중 영상(SWI)에 나타난 위상 마스킹의 효과 분석

*경희대학교 의과대학 강동경희대학교병원 영상의학과, †경희대학교 생체의공학과

황어진* · 김민지* · 김혁기† · 류창우* · 장건호*

이 연구의 목적은 영상의 화소 간 분석(voxel-based analysis)을 이용하여 자화율 가중 영상(SWI)에 나타난 위상 마스킹의 효과를 알아보는 것이었다. 20명의 정상 노인에서 SWI 영상의 정보를 획득하기 위하여 3차원 경사자장 에코 시퀀스를 이용하여 영상을 얻었다. SWI 영상에서의 위상 마스킹의 효과를 관찰하기 위해 원래의 경사자장 크기(magnitude) 영상에 위상 영상을 2번 곱한 SWI2 영상, 4번 곱한 SWI4 영상, 영상 내 정맥 혈관을 강조한 양의 위상 마스크 SWI 영상 (PSWI), 그리고 조직 부분을 강조한 음의 위상 마스크 SWI 영상(NSWI)을 만들었다. paired t-test를 이용한 PSWI와 NSWI간 신호 강도의 차이, SWI2와 SWI4간의 신호강도의 차이, 그리고 경사자장 크기영상 영상과 위상 마스킹에서 얻은 SWI 영상의 신호강도의 차이를 voxel-based 분석으로 수행하였다. 신호 강도 차이는 magnitude과 SWI4 영상 간의 차이가 magnitude과 SWI2 영상 간의 차이보다 더 크게 나왔다. 또한, 신호강도 차이는 magnitude과 PSWI 영상 간의 차이가 magnitude과 NSWI보다 더 많았다. 그리고 NSWI2와 NSWI4간의 신호강도 차이가 PSWI2와 PSWI4간의 신호강도 차이 보다 더 크게 나타났으며, 그리고 NSWI4와 PSWI4간의 신호강도 차이가 NSWI2와 PSWI2간의 신호강도 차이보다 더 크게 나타났다. 위 실험은 화소 간 분석을 통한 SWI 영상 연구가 뇌 전체의 자화율 효과를 볼 때 매우 유용할 것이라는 사실뿐만 아니라, 각기 다른 위상 마스킹 방법을 응용함으로써 선택적으로 정맥 혈관 대비, 혹은 뇌 조직 대비를 강조할 수 있다는 사실을 입증하였다. 그러므로, 자화율 가중 영상의 화소 간 분석은 많은 임상 예에 적용될 수 있을 것이다.

중심단어: 자화율 가중 영상, 위상 마스킹, 화소 간 분석